



Effect of TiO₂ Nanofiber Density on Organic-Inorganic Based Hybrid Solar Cells

A. Boroumandnia^a, A. B. Kasaeian^{*a}, A. R. Nikfarjama, R. Mohammadpour^b

^a Department of New Science & Technologies, University of Tehran, Tehran, Iran

^b Institute for Nanoscience and Nanotechnology, Sharif University of Technology, Tehran, Iran

PAPER INFO

Paper history:

Received 25 October 2013

Received in revised form 23 December 2013

Accepted in 21 January 2014

Keywords:

Hybrid Solar Cell

TiO₂ Nanofiber

Density

Power Conversion Efficiency

Exciton

ABSTRACT

In this work, a comparative study of hybrid solar cells based on P3HT and TiO₂ nanofibers was accomplished. Electrospinning, a low cost production method for large area nanofibrous films, was employed to fabricate the organic-inorganic hybrid solar cells based on poly (3-hexylthiophene) and TiO₂ nanofibers. The performance of the hybrid solar cells was analyzed for four density levels of TiO₂ nanofibers which resulted in the average power conversion efficiency of about 0.0134% under AM 1.5 simulated illuminations (100 mWcm⁻²). It is found that the higher densities of TiO₂ lead to more interface area and generating exciton, so the power conversion efficiency will be increased till the active layer thickness is about 400 nm; but, with increasing thickness more than 400 nm the increasing density did not have positive effect.

doi: 10.5829/idosi.ije.2014.27.07a.15

1. INTRODUCTION

Low-cost semiconductor materials and facile fabrication routes for photovoltaic junctions have been the longstanding goals of photovoltaic materials research. New materials or fabrication procedures which substantially reduce the cost of photovoltaic electricity, can help driving a rapid expansion in the implementation of photovoltaic technology [1]. Although the polymer–fullerene solar cells have obtained 7.4% efficiency, the use of fullerene electron acceptors suffers from poor photo stability and low electron mobility through phase segregation. Replacing the fullerene with inorganic semiconductor nanocrystals as electron acceptors and transport components is an alternative approach, leading to hybrid solar cells. This replacement has the advantages of superior physical and chemical stability, higher electron mobility, facile fabrication property, the ability to engineer interfacial band offsets, and consequently the photovoltage [2-8]. Organic hybrid

solar cells based on semiconductor nanocrystals are among the most promising alternatives to traditional silicon solar cells [2, 9]. Hybrid solar cells have received widespread attention for cost-effective manufacturing, and therefore have the potential to be applied in consumer products because they are thin, light-weight and flexible. Also, these have the capability of low-temperature processing and the simplicity of produce in large-area [1-3, 7, 10-12].

The basic principles of organic–inorganic hybrid solar cells are similar to the bulk heterojunction concept, utilized by p-type conjugated polymers and n-type inorganic semiconductors. Hybrid thin film solar cells based on poly-hexylthiophene (P3HT) and cadmium sulfide (CdS) [13], cadmium selenide (CdSe) [14], titanium oxide (TiO₂) [15], zinc oxide (ZnO) [16], copper indium disulfide (CuInS₂) [17], copper indium diselenide (CuInSe₂) [18] in the forms of nanoparticle, nanowire and nanorod have been developed as the next generation cells. Titanium oxide (TiO₂) has attracted great research interest since it has already been successfully used in dye sensitized solar cells [19]. It has been found that ultrafast photo induced charge transfer could occur at the TiO₂-

*Corresponding Author Email: a.kasa@ut.ac.ir (A. B. Kasaeian)

conjugated polymer interface [20, 21]. Typically, two common approaches have been used to fabricate TiO₂-polymer solar cells. One is to infiltrate conjugated polymer into nanostructured TiO₂ film [22, 23] and the other one is the simultaneous deposition of the blend of polymer and TiO₂ nanocrystals [24, 25].

In the case of the porous TiO₂-polymer system, the current power conversion efficiency (PCE) is still low, although many efforts have been made towards the optimization of the structure of titania network and the architecture of the device [23, 26, 27]. Actually, the fabrication of nano-structured TiO₂ film with controlled pore size and pore distribution together with the complete infiltration of polymer into this network has still been a challenge so far. For the blend of polymer and TiO₂ nanocrystals, the poor electric contact among the TiO₂ particles and the cathode electrode is one serious problem. Therefore, the well aligned one dimensional (1D) TiO₂ arrays that enable a large interfacial area and continuous carrier pathway could be the ideal structure for the hybrid solar cell. However, the growth of TiO₂ nanowires with precised density and size control, and high aspect ratio remains a significant technological challenge [26].

Electrospinning has been developed to be a simple and versatile method to prepare several of continuous 1D fibers, including polymers, ceramics, composites and metals, with diameters down to several nanometers [23]. After the first demonstration of electrospun TiO₂ nanofibers [28], many efforts have been done toward their application in photovoltaic devices since the electrospun nanofibers can be fabricated with controllable size, density and orientation.

More importantly, electrospinning is a low cost production method for large area nanofibrous films. Since area and cost are two important issues for solar cells, electrospinning is a technical idea for the fabrication of hybrid solar cells. In this paper, we studied the hybrid solar cells based on electrospun TiO₂ nanofibers and regioregular P3HT. The effects of TiO₂ nanofibers density and active layer thickness have been surveyed as well.

2. MATERIALS AND METHODS

2. 1. Materials

Glass substrates with FTO electrode were prepared from Solaronix. Titanium tetra isopropoxide (C₁₂H₂₈O₄Ti, 97%), Titanium tetrabutoxide (Ti(OCH₂CH₂CH₂CH₃)₄, 97%), polyvinylpyrrolidone ((C₆H₉NO)_x, M_w 1300000) and Poly 3-hexylthiophene ((C₁₀H₁₄S)_n, M_w/M_n<2.5, M_w : 54000-75000) were purchased from Sigma Aldrich. Acetic acid (CH₃COOH, 100%) and ethanol (C₂H₅OH, 99.9%) were supplied from Merck.

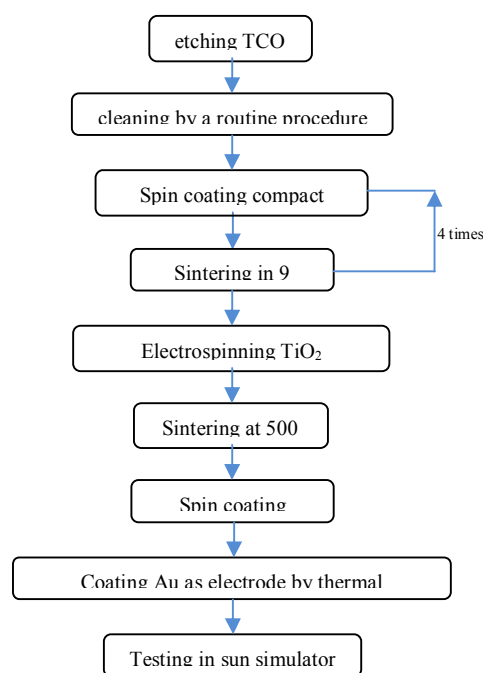


Figure 1. Flowchart of fabrication process

2. 2. Device Fabrication

The general process of fabrication has been shown in Figure 1 and more details explained in resumption. As substrates, glass sheets of 1×1 cm² covered with indium tin oxide (ITO) and fluorine doped tin oxide (FTO) were used with a sheet resistance of 8 Ω/ cm².

The TCO was patterned by etching with mixture of HCl and Zn powder for several minutes. The part of the substrate that forms the contact is covered with Scotch tape, preventing etching. The scotch tape was removed after etching and the substrate cleaned by a routine procedure, which included sonication in detergent followed by repeated rinsing in distilled water, acetone, and isopropanol, in sequence. Cleaned TCO glass is first coated with compact TiO₂ layer by spin coating the sol gel solution (0.25M titanium butoxide in ethanol) at 6000 rpm [6]. The compact TiO₂ layer had some cracks. To fill these cracks, spin coating the sol gel was repeated 4 times. The thickness of each layer was 60 nm. Then, TiO₂ nanofibrous film was prepared on top of the compact layer. The sol gel for spinning nanofibers contained Titanium tetraisopropoxide (0.56 g), acetic acid (0.81 gr), ethanol (2 gr) and PVP (0.76 g). The sol gel was stirred 15 minutes. Sol gel was electrospun onto substrates at a rate of 2 mL/h under an electric field of 20 kV. It was spun in four different densities by controlling the volume of injected sol gel, and then sintered at 500°C for 1 hour by rapid thermal processing to remove organic components and allow nucleation and growth of TiO₂ grains. The thickness of the sintered TiO₂ nanofibrous film was about 200 nm, which is the optimum thickness for the hybrid solar cells [28]. A

layer of P3HT was infiltrated in each TiO₂ nanofibrous film by spin-coating P3HT solution (regioregularity is 50 mg/mL in dichlorobenzene) at 1500 rpm for 30 s and subsequent thermal annealing at 100°C for 20 min in a glove box filled with high purity nitrogen. Then, 40 nm gold electrode is evaporated on top of the film through a shadow mask by using a thermal evaporator. Figure 2 shows the schematic structure and energy level diagram of the hybrid solar cell.

2. 3. Characterization The TiO₂ compact layer and active layer prepared on glass substrates were used for profilometry. Profilometry was performed on DEKTAK3 instrument. Also, the TiO₂ nanofibers prepared by electrospinning on glass substrates were used for the purpose of XRD and spectroscopic characterizations. The XRD operation was carried out on a Bruker D8-Discover instrument. Ultraviolet–vis (UV–vis) absorption spectra were recorded on a HR 4000 CG-UV-NIR spectrophotometer (wavelength range 100–1000 nm). The morphology and structure of the nanofibers were characterized using scanning electron microscopy (SEM, HITACHI S41-60) with an accelerating voltage of 10 kV. Performance of photovoltaic cells was measured using a calibrated AM 1.5 solar simulator under white light with intensity of 100 mW/cm².

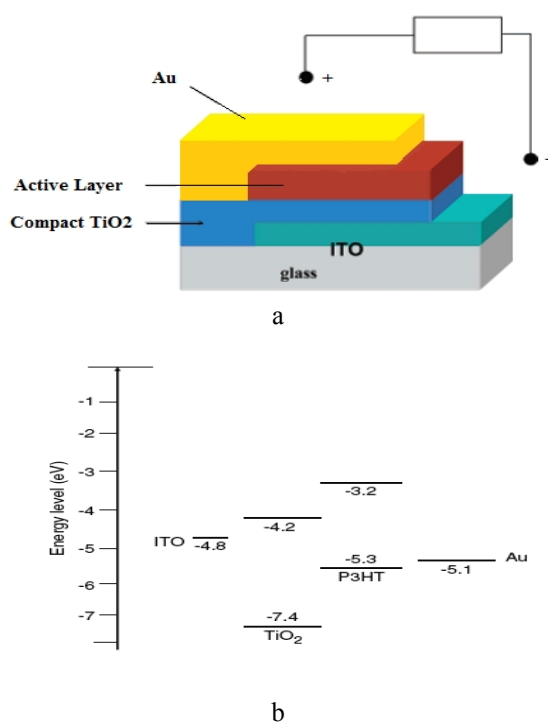


Figure 2. a) Schematic structure of a TiO₂/P3HT hybrid solar cell, b) energy level diagram

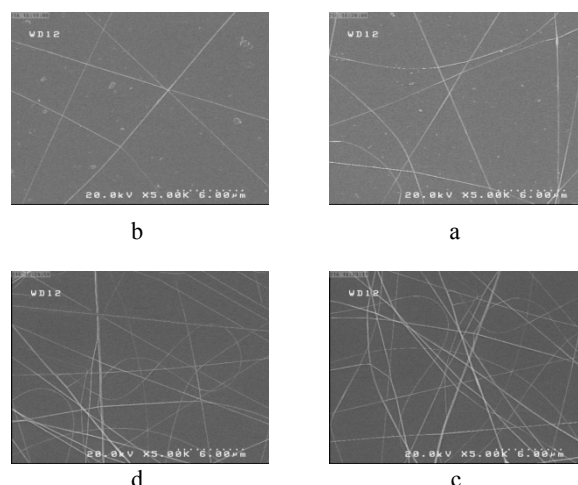


Figure 3. SEM images of TiO₂ nanofibers in different density

3. RESULTS AND DISCUSSIONS

We introduced TiO₂ nanofibers as the n-type inorganic semiconductor and P3HT as the p-type organic semiconducting polymer in the organic-inorganic hybrid solar cell. The morphology of TiO₂ nanofibers is shown in Figure 3 as an SEM image. We could observe the average diameter of nanofibers was in the range of 60–100. As Figure 3 shows, four densities of nanofibers from low (a) to high (d) have been fabricated for analyzing the effect of the density of nanofiber on cell's performance. These different densities have been made by controlling the volume of sol gel injected in the electrospinning system. With increasing density, the thickness of active layer will grow too.

Figure 4 demonstrates the diffractogram of TiO₂ nanofibers which are collected on an FTO substrate. Also, the corresponding anatase and rutile patterns are included for comparison. On an FTO substrate, the bare TiO₂ shows a mixture of anatase/rutile phases. The crystallographic compositions are calculated using the following equation [29]:

$$\text{Content of anatase} = P_A / (1.265 * P_R + P_A) \quad (1)$$

where, P_A and P_R are the main peak intensities of anatase and rutile crystalline phases, respectively. The achieved TiO₂ phase contains 53% anatase and 47% rutile. Zhang et al., have compared the electrical properties of rutile and anatase TiO₂ and proved that, while TiO₂ in its anatase phase is highly conductive, it is highly resistive in its rutile crystalline structure [28]. Higher amount of O_{vac} can be formed in anatase in comparison with rutile. This is the reason why anatase crystalline phase shows higher conductivity and better photocatalytic properties.

The optical density of various layers of the solar cell is shown in Figure 5. The preliminary P3HT exhibits broad absorption spectrum peaking at about 520 nm and another absorption peaks at around 300 nm. With TiO₂ nanofibers, the optical density of P3HT:TiO₂ active layer was slightly increased. This result shows that the incorporation of TiO₂ nanofibers into P3HT does not lead to degrade the optical quality of the composite films.

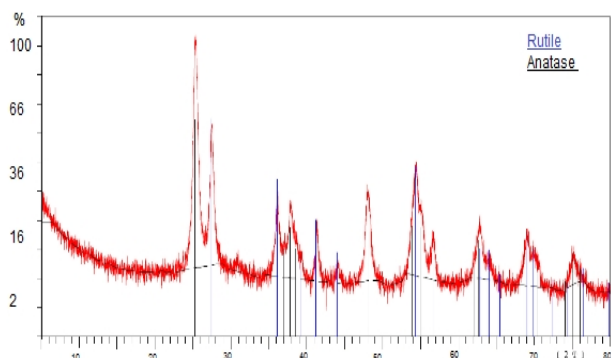


Figure 4. XRD patterns of TiO₂ nanofibers in maximum density

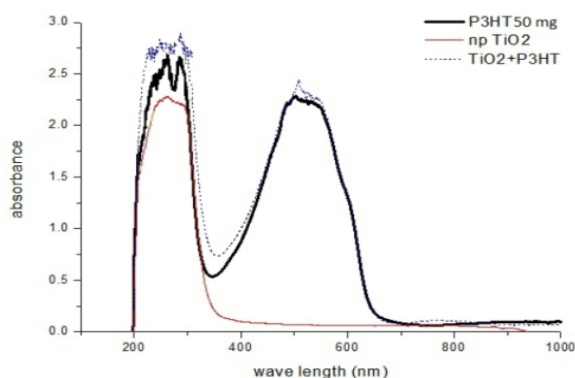


Figure 5. UV-vis absorbance spectra of the solar cell with P3HT:TiO₂ active layer.

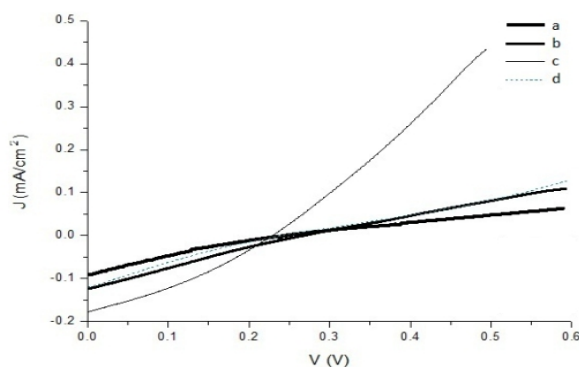


Figure 6. Current density-voltage curves for TiO₂:P3HT nanocomposite films. Spinning sol gel in volume: a) 0.025 ml b) 0.05 ml c) 0.075 ml d) 0.1 ml

TABLE 1. Characteristic parameters of cell with structure FTO/TiO₂/TiO₂:P3HT/Au under AM 1.5 illumination.

	active layer thickness (nm)	J _{sc} (mA/cm ²)	V _{oc} (V)	FF	η (%)
a	293	0.092	0.25	0.21	0.0049
b	360	0.125	0.27	0.24	0.0081
c	412	0.179	0.23	0.32	0.0134
d	475	0.121	0.24	0.22	0.0064

Corresponding to the diameter of nanofiber, the thickness of the inorganic layer was between around 300 to 500 nm. We obtained the photovoltaic performances of P3HT with TiO₂ nanofibers in four fiber densities as shown in Table 1 and Figure 6. The enhanced current density in P3HT composite films with TiO₂ nanofibers was obtained by incorporation of enough amounts of TiO₂ nanofibers. This is achieved by an effective electron transfer via n-type semiconducting TiO₂ nanofibers to anode through increasing the density and the effective area between the organic and inorganic phase in the active layer to generate more electron hole from excitons [1].

Since, exciton generation occurs in the interface of two phases, so more density of fibers in a constant thickness (lower than 400 nm) is ideal. The main limiting factor is suboptimum nanostructure morphology; which it causes too little of the polymer volume lies within an exciton diffusion length between two adjacent fibers. Thus, fibers with lower diameter form denser and thinner layer with more interfaces than squatty fibers. The values of J_{SC}, V_{OC}, FF and power conversion efficiency are presented in Table 1. The power conversion efficiencies of the devices are remained in low values in this work in which P3HT has been used as an active layer of the organic solar cell. However, the device performances such as J_{SC}, V_{OC} and FF can be slightly enhanced with the modification of TiO₂ nanofibers with dye. However, the device performances such as J_{SC}, V_{OC} and FF can be slightly enhanced with the modification of TiO₂ nanofibers with dye. In addition, the diameter of TiO₂ fiber and its crystallinity will affect the performance, which can be analyzed in future researches.

4. CONCLUSION

In this study, TiO₂ nanofibers and P3HT composite layer has been fabricated as an active layer for solar cells. Also, the optimized thickness of TiO₂ nanofibers layer was clarified by the SEM image which has been obtained in the range of 300-400 nm. We can state that the roles of TiO₂ nanofibers into P3HT are much significant, since the fibers make active layers and prepare more specific area. For improving performance,

we will analyze the effect of N719 dye as a modifier and PEDOT:PSS layer in future investigations.

5. REFERENCES

- Boucle, J., P. Ravirajanac, J. Nelson, "Hybrid polymer-metal oxide thin films for photovoltaic applications", *Materials Chemistry*, Vol. 17, (2007), 3141-53.
- Choi Y-J., H-H. Park, S. Golledge, D. Johnson, "A study on the incorporation of ZnO nanoparticles into MEH-PPV based organic-inorganic hybrid solar cells", *Ceramics International*, Vol. 38, (2012), 525-528.
- Yen Yu, Y., W-C. Chien, Y-H. Ko, S-H. Chen, "Preparation and characterization of P3HT:CuInSe₂: TiO₂ thin film for hybrid solar cell applications", *Thin Solid Films*, Vol. 520, (2011), 1503-1510.
- Mikroyannidis J-A., M. Stylianakis, P. Suresh, G-D. Sharma, "Efficient hybrid bulk heterojunction solar cells based on phenylenevinylene Copolymer perylene bisimide and TiO₂", *Solar Energy Materials & Solar Cells*, Vol. 93, (2009), 1792-1800.
- Vandewal K., L. Goris, I. Haeldermans, M. Nešládek, K. Haenen, "Fourier-Transform Photocurrent Spectroscopy for a fast and highly sensitive spectral characterization of organic and hybrid solar cells", *Thin Solid Films*, Vol. 516, (2008), 7135-7138.
- Tai Q., X. Zhaob, F. Yan, "Hybrid solar cells based on poly(3-hexylthiophene) and electrospun TiO₂ nanofibers with effective interface modification", *Materials Chemistry*, Vol. 20, (2010), 7366-7371.
- Lu S., L. Zeng, T. Wub, B. Ren, J. Niu, H. Liu, X. Zhao, J. Maoa, "Efficient hybrid carboxylated polythiophene/nanocrystalline TiO₂ heterojunction solar cells", *Solar Energy*, Vol. 85, (2011), 1967-1971.
- Lee J., J-Y. Jho, "Fabrication of highly ordered and vertically oriented TiO₂ nanotube arrays for ordered heterojunction polymer/inorganic hybrid solar cell", *Solar Energy Materials & Solar Cells*, Vol. 95, (2011), 3152-3156.
- Honghong F., M. Choi, W. Luan, Y-S. Kim, S-T. Tu, "Hybrid solar cells with an inverted structure: Nanodots incorporated ternary system", *Solid-State Electronics*, Vol. 69, (2012), 50-54.
- Huang J-S., C-Y. Chou, C-F. Lin, "Enhancing performance of organic-inorganic hybrid solar cells using a fullerene interlayer from all-solution processing", *Solar Energy Materials & Solar Cells*, Vol. 94, (2010), 182-186.
- Geng, H., M. Wang, S. Han, R. Peng, "Enhanced performance of hybrid photovoltaic devices via surface-modifying metal oxides with conjugated polymer", *Solar Energy Materials & Solar Cells*, Vol. 94, (2010), 547-553.
- El-Nahass M-M., H-M. Zeyadab, K-F. Abd-El-Rahmana, A-A. Darwish, "Fabrication and characterization of 4-tricyanovinyl-N,N-diethylaniline/ p-silicon hybrid organic-inorganic solar cells", *Solar Energy Materials & Solar Cells*, Vol. 91, (2007), 1120-1126.
- Jiang X., F. Chen, W.M. Qiu, Q.X. Yan, Y.X. Nan, H. Xu, L.G. Yang, H.Z. Chen, "Effects of molecular interface modification in CdS/polymer hybrid bulk heterojunction solar cells", *Solar Energy Materials & Solar Cells*, Vol. 94, (2010), 2223-2229.
- Truong N.T.N., W.K. Kim, C. Park, "Improvement of CdSe/P3HT bulk hetero-junction solar cell performance due to ligand exchange from TOPO to pyridine", *Solar Energy Materials & Solar Cells*, Vol. 95, (2011), 3009-3014.
- Lira-Cantu M., A. Chafiq, J. Faissat, I. Gonzalez-Valls, Y.H. Yu, "Oxide/polymer interfaces for hybrid and organic solar cells: Anatase vs. Rutile TiO₂", *Solar Energy Materials & Solar Cells*, Vol. 95, (2011), 1362-1374.
- Ferreira S.R., R.J. Davis, Y.J. Lee, P. Lu, J.W.P. Hsu, "Effect of device architecture on hybrid zinc oxide nanoparticle:poly(3-hexylthiophene) blend solar cell performance and stability", *Organic. Electronic*, Vol. 12, (2011), 1258-1263.
- Gevorgyan S. A. , "An inter-laboratory stability study of roll-to-roll coated flexible polymer solar modules", *Solar Energy Materials and Solar Cells*, Vol. 95, (2011), 1398-1416.
- Arici E., H. Hoppe, F. Schaffler, D. Meissner, M.A. Malik, N.S. Sariciftci, "Hybrid solar cells based on inorganic nanoclusters and conjugated polymers", *Thin Solid Films*, Vol. 451, (2004), 612-618.
- Kavan L, J Rathouský, M Grätzel, V Shklover, "A Zukal, Mesoporous thin film TiO₂ electrodes", *Microporous and Mesoporous Materials*, Vol. 44, (2001), 653-659.
- Van Hal P. A., M. P. T. Christiaans, M. M. Wienk, J. M. Kroon, and R. A. J. Janssen, "Photoinduced electron transfer from conjugated polymers onto TiO₂", *Synthetic Metals*, Vol. 101, (1999), 4352-4359.
- Van Hal P.A., M.M. Wienk, J.M. Kroon, W.J.H. Verhees, L.H. Slooff, W.J.H. Van Gennip, P. Jonkheijm, R.A.J. Janssen, "Photoinduced electron transfer and photovoltaic response of a MDMO-PPV: TiO₂ bulk-heterojunction", *Adv. Mater*, Vol. 15, (2003), 118-121.
- McGehee D. , Karl Leo, Moritz Riede, "Probing the effect of substrate heating during deposition of DCV4T:C₆₀ blend layers for organic solar cells", *Organic Electronics*, Vol. 13, (2011), 623-631.
- Lancelle-Beltran A., P. Prene, C. Boscher, P. Belleville, P. Buvat, S. Lambert, F. Guillet, C. Boissiere, D. Grosso and C. Sanchez, "Nanostructured hybrid solar cells based on self-assembled mesoporous titania thin films" *Chem. Mater*, Vol. 18, (2006), 6152-6156.
- Kwong C.Y., A.B. Djuris'ic, P.C. Chui, K.W. Cheng, W.K. Chan, "Influence of solvent on film morphology and device performance of poly(3-hexylthiophene): TiO₂ nanocomposite solar cells", *Chem. Phys. Lett*, Vol. 384, (2004), 372-375.
- Lin Y. Y., T. H. Chu, S. S. Li, C. H. Chuang, C. H. Chang, W. F. Su, C. P. Chang, M. W. Chu and C. W. Chen, J. Am. "interfacial nanostructuring on the performance of polymer/TiO₂ nanorod bulk heterojunction solar cells", *American Chemical Society*, Vol. 131, (2009), 3644-3649.
- Williams S.S., M.J. Hampton, V. Gowrishankar, I.K. Ding, J.L. Templeton, E.T. Samulski, J.M. DeSimone, M.D. McGehee, "Nanostructured titania polymer photovoltaic devices made using PFPE-based nanomolding techniques", *Chem.Mater*, Vol. 20, (2008), 5229-5234.
- Paek Mi-Jeong, Tae Woo Kim, Seong-Ju Hwang, "Effects of hydronium intercalation and cation substitution on the photocatalytic performance of layered titanium oxide", *Journal of Physics and Chemistry of Solids*, Vol. 69, (2008), 1444-1446.
- Zhang S.X., D.C. Kundaliya, W. Yu, S. Dhar, S.Y. Young, L.G. Salamanca-Riba, S.B. Ogale, R.D. Vispute, T. Venkatesan, "Niobium doped TiO₂: intrinsic transparent metallic anatase versus highly resistive rutile phase", *Applied Physics*, Vol. 102, (2007), 013701.
- Biao W., Z. YuDong, H. LiMing, C. JunSheng, G. FengLi, L. Yun, W. LiJun, "Improved and excellent CO sensing properties of Cu-doped TiO₂ nanofibers", *Chinese Science Bulletin*, Vol 55, (2010), 228-232.

Effect of TiO₂ Nanofiber Density on Organic-Inorganic Based Hybrid Solar Cells

RESEARCH NOTE

A. Boroumandnia^a, A.B. Kasaeian^a, A.R. Nikfarjam^a, R. Mohammadpour^b

^a Department of New Science & Technologies, University of Tehran, Tehran, Iran

^b Institute for Nanoscience and Nanotechnology, Sharif University of Technology, Tehran, Iran

PAPER INFO

چکیده

Paper history:

Received 25 October 2013

Received in revised form 23 December 2013

Accepted in 21 January 2014

Keywords:

Hybrid Solar Cell

TiO₂ Nanofiber

Density

Power Conversion Efficiency

Exciton

در این تحقیق، بررسی مقایسه‌ای روی سلول خورشیدی هیبریدی ساخته شده بر پایه پلی‌مر P3HT و دی‌اکسیدتیتانیوم انجام شده است. برای تولید فیلم نانوفیبر در سطح وسیع به منظور ساخت سلول خورشیدی آل-معدنی بر پایه P3HT و نانوفیبر دی‌اکسیدتیتانیوم از یک روش کم هزینه به نام الکتروریسی استفاده شده است. عملکرد سلول‌های هیبریدی خورشیدی در چهار سطح تراکم نانوفیبر دی‌اکسیدتیتانیوم بررسی شده است که نتیجه آن راندمان تبدیل توان ۰/۰۱۳۴ درصد در شرایط تابشی AM 1.5 می‌باشد. سلول‌های ساخته شده با تراکم‌های بیشتر نانوفیبر دی‌اکسیدتیتانیوم به دلیل دارا بودن سطح تماس بیشتر دو فاز و در نتیجه تولید اکسایتون بیشتر، راندمان تبدیل توان بیشتری دارند. البته، رابطه افزایش توان با افزایش تراکم تا جایی است که ضخامت لایه فعال حدود ۴۰۰ نانومتر باشد. با افزایش ضخامت لایه فعال به بیش از ۴۰۰ نانومتر افزایش تراکم اثر مثبت نخواهد داشت.

doi: 10.5829/idosi.ije.2014.27.07a.15